Ethynyl thiophene-appended unsymmetrical zinc porphyrin sensitizers for dye-sensitized solar cells

Post-print of a peer-reviewed article published by the Royal Society of Chemistry.
Published article available at: http://dx.doi.org/10.1039/C3RA47948J

Cite as:
Reeta, P. S., Giribabu, L., Senthilarasu, S., Hsu, M-H., Kumar, D. K., Upadhyaya, H. M., Robertson, N., Hewat, T. (2014). Ethynyl thiophene-appended unsymmetrical zinc porphyrin sensitizers for dye-sensitized solar cells. *RSC Advances*, *4*(27), 14165-14175.

Manuscript received: 24/12/2014; Accepted: 27/01/2014; Article published: 30/01/2014

Ethynyl thiophene-appended unsymmetrical zinc porphyrin sensitizers for dye-sensitized solar cells**

P. Silviya Reeta,[1] L. Giribabu,[1,*] S. Senthilarasu,[2,3] Min-Hung Hsu,[2] D. Kishore Kumar,[2] Hari M. Upadhyaya,[2] Neil Robertson[4] and Tracy Hewat[4]

[1]Inorganic & Physical Chemistry Division, CSIR-Indian Institute of Chemical Technology, Uppal Road, Tarnaka, Hyderabad 500007, India.

[2]Energy Conversion Laboratory (ECL), Institute of Mechanical, Process and Energy Engineering (IMPEE), School of Engineering and Physical Sciences, Heriot-Watt University, Riccarton, Edinburgh, UK.

[3]Environment and Sustainability Institute (ESI), University of Exeter, Penryn, Cornwall, UK.

[4]EaStCHEM, School of Chemistry, Joseph Black Building, University of Edinburgh, West Mains Road, Edinburgh, EH9 3FJ, UK.

[*]Corresponding author; e-mail: giribabu@iict.res.in; fax: +91-40-27160921; tel: +91-40-27193186

[**]The authors are thankful to DST-EPSRC (UK) ('APEX') programme and the EPSRC supergen programme for financial support of this work. This work has made use of the resources provided by the EaStChem Research Computing Facility (http://www.eastchem.ac.uk/rcf). This facility is partially supported by the eDIKT initiative (http://www.edikt.org).

Graphical abstract:

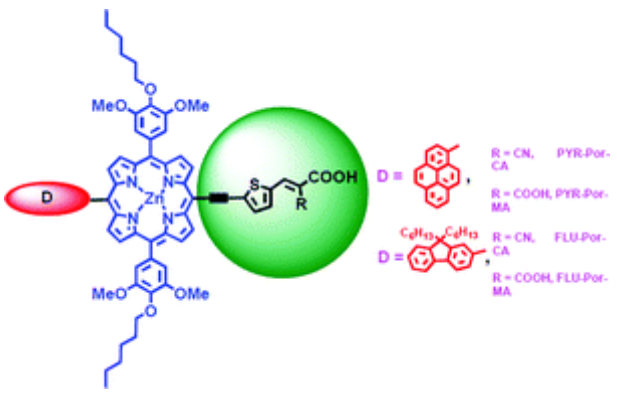

RSC Advances

RSCPublishing

ARTICLE

Four unsymmetrical porphyrins of A2B donor-π-acceptor type have been designed, synthesized, characterized and their photovoltaic properties explored. Polycyclic aromatic hydrocarbons (**PAH**) such as either pyrene or fluorene acts as donor, the porphyrin is the π-spacer, appended with an ethynyl thiophene linker and either cyanoacrylic acid or malonic acid acts as acceptor. All compounds were characterized by ^{1}H NMR and mass spectrometry. UV-Vis absorption spectra and B or Soret (λ_{ex} at 440nm for all the four sensitizers reported) band-excited fluorescence emission spectra were also obtained. Electrochemical properties suggest that the first oxidation is ring centred and this is supported by *in-situ* spectro-electrochemical and DFT computational studies. The synthesized porphyrins were applied in dye-sensitized solar cells (DSSCs). Up to 3.14% conversion efficiency was realized for **PYR-Por-MA** under our experimental conditions.

Introduction

The increasing global energy crisis has demanded the search for new alternative energy conversion materials as competitors of silicon photovoltaic devices.[1] In this regard, dye-sensitized solar cells (DSSCs) are found to display low-cost, ease of fabrication, short-energy pay-back time, low sensitivity to temperature changes and environmental friendliness compared with the conventional solid-state *p–n* photovoltaic devices.[2-8] Typical DSSC consists of a dye-sensitized nanocrystalline semiconductor sandwiched between the platinum-coated counter electrode within which is the redox electrolyte of the type I^-/I_3^-. The sensitizer is one of the key component in achieving high efficiency and durability of the device. The most widely studied sensitizers employed so far are Ru(II) polypyridyl complexes (N719, N3, N945, Z-907) which produced solar-energy-to-electricity conversion efficiencies (η) more than 11%.[9-12] In spite of this high conversion efficiency, the main drawbacks of Ru(II) polypyridyl complexes are the expense due to the rarity of the metal in earth's crust and lack of absorption in near-IR region of the visible spectrum, where the solar flux of photons is still significant, thus limiting the realization and usability of highly-efficient devices. For this reason, dyes with large π-conjugated systems such as porphyrins and phthalocyanines are receiving considerable attention as sensitizers for DSSC applications.[13,14]

A great variety of porphyrin sensitizers[15-26] used for DSSC applications comprise the anchoring group either at the pyrrole-β (η up to 7.1%)[19] or *–meso* position/s (η up to 12.3%)[26]. Consistent with recent reports, unsymmetrical porphyrin sensitizers designed with unique directionality have proven to be promising alternatives and competitive with conventional Ru(II) polypyridyl complexes. Enormous effort has been put forth in recent years to advance the existing highest power conversion efficiency by various structural modifications at *–meso* positions of porphyrin macrocycles by adopting donor-π-acceptor approach (D-π-A).[22-27] Recently, Yella *et al*. a porphyrin sensitizer (***YD-o-C8***) having N,N'-diphenyl amine as donor, porphyrin macrocycle as acceptor and aryl benzoxy group as acceptor, with highest η value of 12.3% using a Co(II)/Co(III) based redox electrolyte.[26] This has stimulated further investigations of porphyrin based sensitizers in order to enhance the photovoltaic performance of DSSC devices.

The performance of porphyrin sensitizers can be significantly improved by grafting the molecule with precisely chosen donor, π-linker and acceptor/anchoring groups (D-π-A approach).[22-27] According to previous reports, combination of a wide-range of donor moieties, mainly such as functionalized arylamines, polyaromatic or heterocyclic donors, with ethynyl benzoic acid anchoring group at the *-meso* position of the porphyrin has revealed significantly-improved cell performance.[28,29] In contrast to many available porphyrin sensitizers reported with ethynyl benzoic acid anchoring group, in the present scheme, we have attempted to introduce an ethynyl thiophene π-conjugated linker with either cyanoacrylic or malonic acid anchoring groups and study its influence on solar cell performance. Herein in the present article, we report four new unsymmetrical zinc metallated porphyrin sensitizers (**PYR-Por-CA**, **PYR-Por-MA**, **FLU-Por-CA** and **FLU-Por-MA**), as shown in Figure 1, appended with ethynyl thiophene linker between porphyrin and anchoring group to facilitate shift in the absorption towards the red region, and either cyanoacrylic or malonic acid anchoring group and a polycyclic aromatic hydrocarbon (PAH) such as either pyrene or fluorene as the donor moiety.[22-27,30]

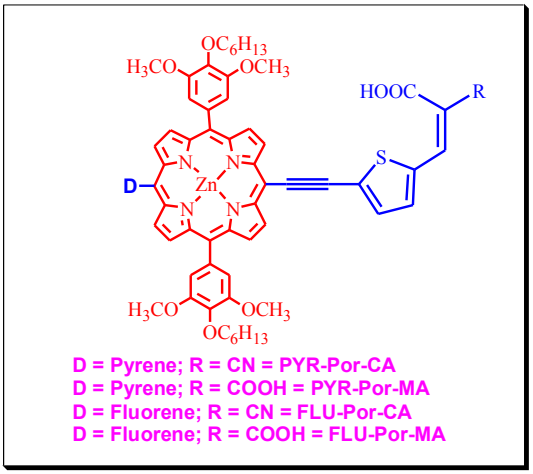

Figure 1: Molecular structure of porphyrin sensitizers.

All four sensitizers have been characterized by elemental analysis, MALDI-MS, IR, UV-Visible and fluorescence spectroscopies (both steady-state and time resolved) as well as electrochemical methods

Experimental
General

Chemical reagents and catalysts used in the reactions were of Analytical reagent grade (AR), purchased from Sigma-Aldrich (India) and were used without further purification. All the reactions were performed using dried and distilled solvents of laboratory reagent (LR) grade. The solvents $CHCl_3$, CH_2Cl_2 and triethylamine (TEA) were dried over CaH_2. Toluene was dried over sodium chunks overnight and distilled under nitrogen atmosphere. Purification of compounds by column chromatography was performed on ACME Silica Gel (100-200 mesh).

Synthesis

Dipyrromethane, 4,4,5,5-tetramethyl-2-(pyren-1-yl)-1,3,2-dioxaborolane and 2-(9,9-dihexyl-9H-fluoren-2-yl)-4,4,5,5,-tetramethyl-[1,3,2]dioxaborolane, were prepared according to the literature reported procedure.[28,29,31]

5-pyrenyl-10,20- Bis[4-(hexyloxy)-3,5-dimethoxypheyl]porphyrin (**5a**): Monobromo porphyrin (**4**) (190 mg, 0.24 mmol) was dissolved in 40 ml of dry Toluene, to which $CsCO_3$ (393.6 mg, 1.2 mmol), $Pd(PPh_3)_4$ (0.25 equivalents) and 1-pyrenylborane (218 mg, 0.713 mmol) were added and the reaction mixture was refluxed under nitrogen atmosphere for 12 h. After cooling to room temperature (RT, 25°C), the crude mixture was purified using silica gel column with ethylacetate/hexane (1:4 v/v) to afford the desired product (90% yield). Elemental analysis of Anal. Calcd. For $C_{64}H_{62}N_4O_6$% (983.20): C, 78.18; H, 6.36; N, 5.70. Found: C, 78.20; H, 6.33; N, 5.68. ESI-MS (m/z): $C_{64}H_{62}N_4O_6$ [983.20]: $[M+1H]^+$ 984 (100%). ^1H NMR ($CDCl_3$, δppm): 10.25 (s, 1H), 9.37 (d, 2H), 9.14 (d, 2H), 8.90 (dd, 2H), 8.70 (s, 1H), 8.46 (m, 6H), 8.05 (m, 2H), 7.45 (m, 6H), 4.28 (m, 4H), 3.95 (s, 12H), 1.99 (m, 4H), 1.55 (m, 12H), 0.97 (m, 6H), -2.78 (b, 2H). UV-Vis (CH_2Cl_2) λ_{max} (nm) (log ε M^{-1} cm^{-1}) : 419 (5.81), 511 (4.44), 547(3.85), 584 (3.81), 640 (3.33).

*5-fluorenyl-10,20- Bis[4-(hexyloxy)-3,5-dimethoxypheyl]porphyrin (**5b**):* This compound was synthesized by adopting a similar procedure that was used to prepare **5a** in 87% yield. ^1H NMR($CDCl_3$, 300MHz): δppm = 2.95 (s, 2H), 0.78 (m,12H), 0.98 (m, 8H), 1.25 (m, 8H), 1.45 (m, 10H), 1.60 (m, 4H), 2.1 (m, 8H), 3.95 (s, 12H), 4.31(t, 4H), 7.50 (m, 7H), 7.91-8.29 (m, 4H), 8.94(d, 4H), 9.13(d, 2H), 9.35 (s, 2H), 10.21 (s, 1H). ESI-MS: *m/z* $C_{73}H_{86}N_4O_6$: calculated : 1115.49, found : 1115 $[M^+]$. UV-Vis (CH_2Cl_2) λ_{max}(nm) (log ε): 272 (1.5), 306 (4.4), 418 (5.9), 512 (4.3), 547 (3.9), 587 (3.8), 641(3.5).

5-pyrenyl-15-ethynyl-10,20-Bis[4-(hexyloxy)-3,5-dimethoxypheyl] porphyrin zinc(II) (**9a**): Porphyrin (**8a**) (65mg, 0.057mmol) and K_2CO_3 (0.5g) were dissolved in 30 ml of CH_2Cl_2/MeOH mixture and allowed to stir at RT for 5h. The crude mixture was filtered to remove K_2CO_3, washed with water and extracted with $CHCl_3$. Purification by silica gel column using $CHCl_3$/Hexane (4:1 v/v) afforded a more polar green product (90% yield). Elemental analysis of Anal. Calcd. For $C_{66}H_{60}N_4O_6Zn$% (1068.4): C, 74.04; H, 5.65; N, 5.23. Found: C, 74.00; H, 5.68; N, 5.20. ESI-MS (m/z): $C_{66}H_{60}N_4O_6Zn$ [1093]: $[M+Na]^+$ (100). ^1H NMR ($CDCl_3$, δppm): 9.82 (d, 2H), 9.12 (d, 2H), 8.80 (dd, 2H), 8.70 (s, 1H), 8.46 (m, 6H), 8.05 (m, 2H), 7.45 (m, 6H), 4.23 (m, 4H), 3.91 (s, 12H), 1.93 (m, 4H), 1.44 (m, 12H), 0.97 (m, 6H). UV-Vis (CH_2Cl_2) λ_{max} (nm) (log ε M^{-1} cm^{-1}): 431(5.85), 557(4.54), 599(4.13).

*5-fluorenyl-15-ethynyl-10,20-Bis[4-(hexyloxy)-3,5-dimethoxypheyl] porphyrin zinc(II) (**9b**)*: This compound was synthesized by adopting a similar procedure that was used to prepare **9a** in 91% yield**.** ^1H NMR($CDCl_3$, 300MHz): δ = 0.86 (m,12H), 0.99(m, 8H), 1.44(m,8H), 1.55(m, 10H), 1.65 (m, 4H), 1.99 (m, 4H), 2.11 (m, 4H), 3.67 (s, 1H), 3.93(s, 12H), 4.33(t, 4H), 7.46(m, 7H), 7.90-8.25 (m, 4H), 8.98 (d, 4H), 9.12 (d, 2H), 9.45 (s, 2H). ESI-MS: *m/z* $C_{75}H_{84}N_4O_6Zn$: calculated : 1202.90 , found : 1204 $[(M+2H)^+]$. UV-Vis(CH_2Cl_2) λ_{max}(nm) (log ε) : 267 (4.5), 308 (4.4), 430(5.7), 557(4.3), 600 (5.0).

5-pyrenyl-15-(5-formylthiophene-2-yl)-10,20-Bis[4-(hexyloxy)-3,5-dimethoxypheyl]porphyrin zinc(II) (**10a**): Porphyrin **9a** (50 mg, 0.047 mmol) and $Pd(PPh_3)_2Cl_2$ (5,75 mg ,0.005 mmol) were dissolved in 10 ml of dry triethylamine to which 5-bromothiophene-2-carboxaldehyde (44.16 mg, 0.025 ml, 0.23 mmol) and CuI (0.95 mg, 0.005 mmol) were added and the solution was heated to 50 °C for 8h. After cooling to RT the crude mixture was washed with water and extracted with $CHCl_3$. The green product was purified using silica gel column with $CHCl_3$/Hexane (3:1 v/v) as the eluant to afford the desired product (85% yield). Elemental analysis of Anal. Calcd. For $C_{71}H_{62}N_4O_7SZn$% (1180.72): C, 72.22; H, 5.29; N, 4.75. Found: C, 72.20; H, 5.30; N, 4.70. ESI-MS (m/z): $C_{71}H_{62}N_4O_7SZn$ [1180.72]: 1182 $[M+2H]^+$ (100%). ^1H NMR ($CDCl_3$, δppm): 10.11 (s, 1H), 9.90 (d, 1H), 9.77 (s, 1H), 9.20 (d, 2H), 8.77 (m, 3H), 8.50 (m, 6H), 8.21 (m, 2H), 7.83 (m, 4H), 7.45 (m, 7H), 6.90 (s, 1H), 4.22 (m, 4H), 3.93 (s, 12H), 1.93 (m, 4H), 1.44 (m, 12H), 0.97 (m, 6H). UV-Vis (CH_2Cl_2) λ_{max} (nm) (log ε M^{-1} cm^{-1}) : 426(5.83), 454(4.83), 566(3.82), 623(4.00).

*5-fluorenyl-15-(5-formylthiophene-2-yl)-10,20-Bis[4-(hexyloxy)-3,5-dimethoxypheyl] porphyrin zinc(II) (**10b**)*: This compound was synthesized by adopting a similar procedure that was used to prepare **10a** in 83% yield**.** ^1H NMR($CDCl_3$, 300MHz): δ = 0.87 (m,12H), 0.99(m, 8H), 1.43 (m,8H), 1.56(m, 10H), 1.63 (m, 4H), 2.00 (m, 4H), 2.12 (m, 4H), 3.92(s, 12H), 4.28 (t, 4H), 7.15 (d, 1H), 7.35 (d, 1H), 7.44(m, 7H), 7.92-8.23 (m, 4H), 9.03 (m, 4H), 9.48 (d, 2H), 9.54(s, 2H), 9.64 (s, 1H). ESI-MS: *m/z* $C_{80}H_{86}N_4O_7SZn$: calculated : 1313.04, found : 1315 $[M+2H]^+$. UV-Vis (CH_2Cl_2) λ_{max}(nm) (log ε) : 267(4.5), 308(4.5), 423(5.6), 453(sh, 5.1), 551(4.2), 621(4.0).

5-pyrenyl-15-[(5-formylthiophene-2-yl)-2-cyanoacrylicacid]-10,20-Bis[4-(hexyloxy)-3,5-dimethoxypheyl]porphyrin zinc(II) **PYR-Por-CA:** Porphyrin **10a** (50 mg, 0.042 mmol) was dissolved in 30 ml of CH_3CN/ $CHCl_3$ (3:1), to which piperidine and cyanoacetic acid (0.21 mmol) were added. The reaction mixture was refluxed for 8h. After cooling to RT, the reaction mixture was washed with water and 0.1M HCl and extracted with CH_2Cl_2. The product was purified with silica gel column using CH_2Cl_2/MeOH (3:1 v/v) as the eluant to afford the desired product (85% yield). Elemental analysis of Anal. Calcd. For $C_{74}H_{63}N_5O_8SZn$% (1247.77): C, 71.23; H, 5.09; N, 5.61 Found: C, 71.25; H, 5.10; N, 5.65. MALDI-MS (m/z): $C_{74}H_{63}N_5O_8SZn$ [1247.77]: 1246 $[M-H]^+$ (100%). ^1H NMR ($CDCl_3$, δppm): 9.67 (s, 2H), 9.08 (s, 2H), 8.73 (m, 4H), 8.29 (m, 6H), 8.11 (m, 2H), 7.36 (m, 8H), 4.17 (m, 4H), 3.85 (s, 12H), 1.93 (m, 4H), 1.44 (m, 12H), 0.97 (m, 6H). UV-Vis (CH_2Cl_2) λmax (nm) (log ε M^{-1} cm^{-1}) : 447(5.32), 575(4.04), 639(4.36).

5-pyrenyl-15-[(5-formylthiophene-2-yl)methylene malonic acid]-10,20-Bis[4-(hexyloxy)-3,5-dimethoxypheyl]porphyrin zinc(II) **(PYR-Por-MA):** This compound was synthesized by analogous procedure of the previous compound. The only difference is that here malonic acid was taken instead of cyanoacrylic acid. Elemental analysis of Anal. Calcd. For $C_{74}H_{64}N_4O_{10}SZn$% (1266.77): C, 70.16; H, 4.49; N, 5.61 Found: C, 70.15; H, 5.10; N, 4.51. MALDI-MS (m/z): $C_{74}H_{64}N_4O_{10}SZn$% (1266.77): [1264] $[M-2H]^+$ (60%). ^1H NMR ($CDCl_3$, δppm): 9.67 (s, 2H), 9.08 (s, 2H), 8.73 (m, 4H), 8.29 (m, 6H), 8.11 (m, 2H), 7.36 (m, 7H), 4.17 (m, 4H), 3.85 (s, 12H), 1.93 (m, 4H), 1.44 (m, 12H), 0.97 (m, 6H). UV-Vis(CH_2Cl_2) λ_{max} (nm) (log ε M^{-1} cm^{-1}) : 468 (5.12), 580 (4.01), 654 (4.46).

5-fluorenyl-15-[(5-formylthiophene-2-yl)-2-cyanoacrylicacid]-10,20-Bis[4-(hexyloxy)-3,5-dimethoxypheyl]porphyrin zinc(II) (**FLU-Por-CA**): This compound was synthesized by adopting a similar procedure that was used to prepare **11a.** ^1H NMR($CDCl_3$, 300MHz): δ = 0.65 (m,8H), 0.82(m, 12H), 1.23 (m,18H), 1.63 (m, 4H), 2.02 (m, 8H), 3.61(s, 12H), 4.23 (m, 4H), 6.85 (d, 2H), 7.42(m, 8H), 7.92-8.05 (m, 4H), 9.03 (m, 4H), 9.61 (m, 4H). MALDI-TOF MS: *m/z* $C_{83}H_{87}N_5O_8SZn$: calculated: 1380.08, found: 1381 $[M+H]^+$. UV-Vis (CH_2Cl_2) λ_{max}(nm)(logε) : 267(4.6), 308(4.5), 444(5.2), 575(4.2), 638(4.5).

5-fluorenyl-15-[(5-formylthiophene-2-yl)methylene malonic acid]-10,20-Bis[4-(hexyloxy)-3,5-dimethoxypheyl]porphyrin zinc(II) (**FLU-Por-MA**): This compound was synthesized by adopting a similar procedure that was used to prepare **12a.** ^1H NMR($CDCl_3$, 300MHz): δ ppm = 0.87 (m,12H), 0.99(m, 8H), 1.22 (m, 17H), 1.63 (m, 4H), 1.98 (m, 8H), 3.92(s, 12H), 4.23 (m, 4H), 7.03(d, 2H), 7.36 (m, 8H), 7.92-8.05 (m, 4H), 8.85 (m, 4H), 9.02 (d, 2H), 9.62(s, 2H). MALDI-TOF MS: *m/z* $C_{83}H_{88}N_4O_{10}SZn$: calculated: 1399.08, found: 1400 $[M+H]^+$. UV-Vis (CH_2Cl_2) λ_{max}(nm)(log ε) : 266 (4.6), 309(4.6), 448 (5.3), 572 (4.2), 632 (4.4).

Methods

The optical absorption spectra were recorded on a Shimadzu (Model UV-3600) spectrophotometer. Concentrations of solutions are ca. 1 x 10^{-6} M for Soret band and 1 x 10^{-5} M for Q band absorption. Steady state fluorescence spectra were recorded (Spex model Fluorlog-3) for solutions having optical density at the wavelength of excitation (λ_{ex}) ≈ 0.11. Time-resolved fluorescence measurements have been carried out using HORIBA Jobin Yvon spectrofluorometer. Briefly, the samples were excited at 650 nm and the emission was monitored at 780 nm. The count rates employed were typically 10^3 – 10^4 s^{-1}. Deconvolution of the data was carried out by the method of iterative reconvolution of the instrument response function and the assumed decay function using DAS-6 software. The goodness of the fit of the experimental data to the assumed decay function was judged by the standard statistical tests (*i.e.*, random distribution of weighted residuals, the autocorrelation function and the values of reduced χ^2).

Cyclic voltammetric measurements were performed on a PC-controlled CH instruments (model CHI 620C electrochemical analyser) using 1 mM unsymmetrical porphyrin solution in dichloromethane (DCM) solvent at scan rate of 100 mV/s with 0.1 M tetrabutyl ammonium perchlorate (TBAP) as a supporting electrolyte. The working electrode was glassy carbon, standard calomel electrode (SCE) was reference electrode and platinum wire was an auxiliary electrode. After a cyclic voltammogram (CV) had been recorded, ferrocene was added, and a second voltammogram was measured. Spectroelectrochemical measurements were performed at a fixed temperature between 233 and 270 K by the optically transparent thin layer electrochemistry (OTTLE) technique in dry CH_2Cl_2 containing 0.3 M [TBA][BF_4] supporting electrolyte using a 2 mm thick quartz cuvette. The conventional three-electrode electrochemical cell consisted of platinum gauze working electrode, platinum wire counter electrode and Ag/AgCl reference electrode (ferrocene $E_{1/2}$ = + 0.63 V). The UV-Vis-NIR spectra were recorded with a Jasco V-670 spectrophotometer. The TG curves of the samples were performed on a thermogravimetric analyzer Mettler Tolledo TGA/SDTA 851^c under nitrogen atmosphere (99.999%) from 25 to 600 ^oC, in Al_2O_3 crucibles. The heating rates were 10 ^oC/min and the flow rate of nitrogen was 80 mL/min.

Cell Fabrication

The commercially available TiO_2 pastes (Dyesol) of 18 nm in diameter were used to prepare nanocrystalline TiO_2 electrodes. DSSCs were prepared on 3 mm thick float glass substrates coated with FTO (TEC-8 from Pilkington Group Limited). These FTO thin films have a sheet resistance of ~8 Ω/sq and an average transmission of ~80% in the Visible and NIR spectral region. The TiO_2 electrodes were made by the screen printing method to prepare transparent layers. Subsequently, a second scattering layer made up of a paste containing 400 nm anatase TiO_2 nanoparticles. As a post deposition treatment the TiO_2 electrodes were annealed at 450°C for a 30 min on a hotplate. The dye molecules were dissolved in ethanol at a concentration of 0.1 x 10^{-3} M. The TiO_2 thin films were soaked in the dye solution and then kept at room temperature for 16 h so that the dye was adsorbed onto TiO_2 films. The TiO_2 electrodes were soaked overnight in dye solution, sandwiched with a platinised conducting counter electrode using a Surlyn frame (Solaronix SA), filled with the electrolyte through a hole in the counter electrode and sealed. The iodide/tri-iodide electrolyte comprising 0.4 M LiI, 0.4 M tetrabutylammonium iodide (TBAI), and 0.04 M I_2 dissolved in 0.3 M *N*-methylbenzimidazole (NMB) in acetonitrile (ACN) and 3-methoxypropionitrile (MPN) solvent mixture at volume ratio of 1:1 was used. The area of the cells was 0.25 cm^2.

Results and Discussions

The synthetic scheme of all porphyrin sensitizers is illustrated in Figure 2 (for detailed synthetic scheme of each compound,

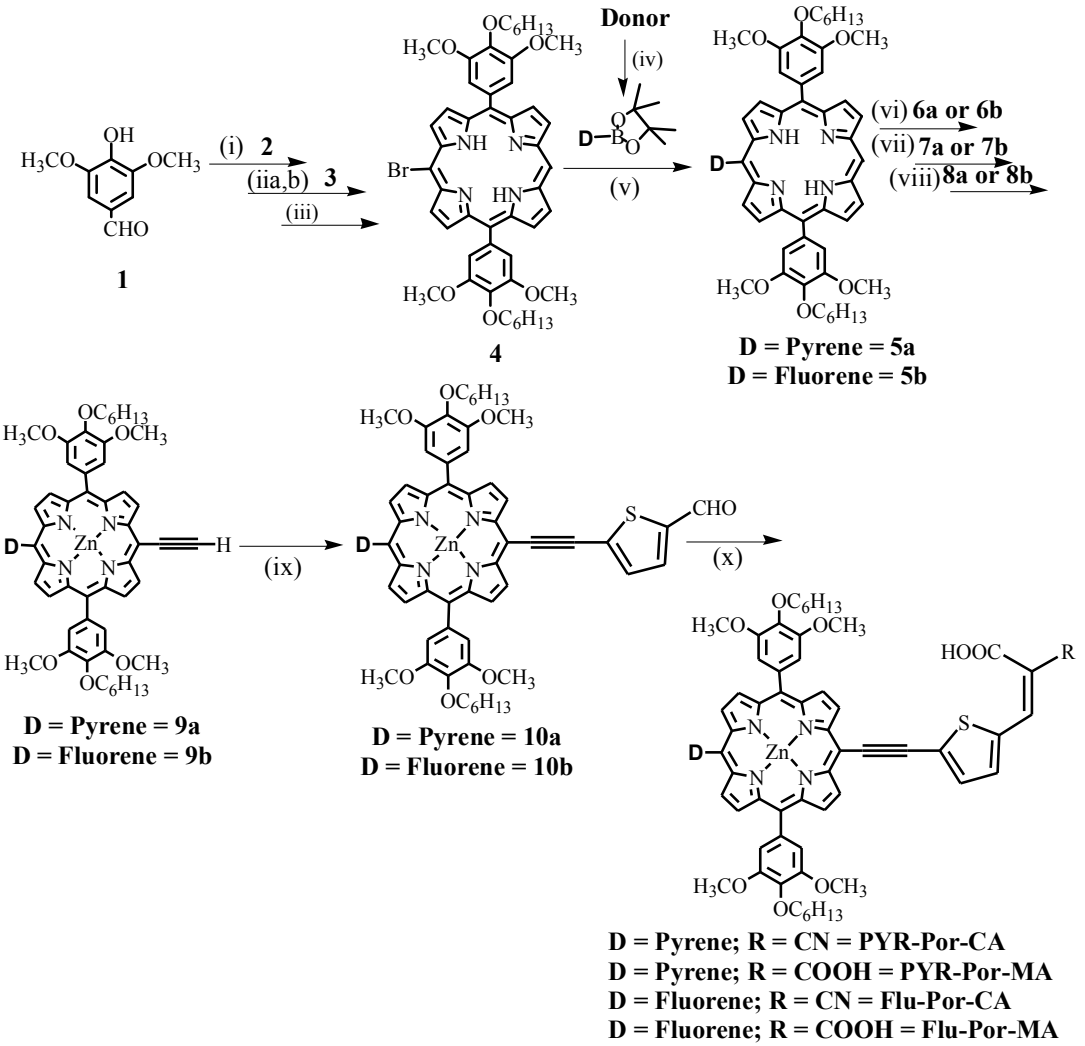

(i) DMF, K_2CO_3, reflux 4h (iia) Dipyrromethane, CH_2Cl_2, TFA, RT (iib) DDQ, TEA, RT (iii) NBS, CH_2Cl_2, RT (iva,b) $Pd(PPh_3)_4$, $Cs(CO)_3$, Toluene, reflux, 12h (va) NBS, CH_2Cl_2, RT (vb) $Zn(OAc)_2$, $CHCl_3/CH_3OH$, reflux, 2h (vi) TMSA, TEA, $Pd(PPh_3)_2Cl_2$, CuI, 50 ^oC, 8h (vii) K_2CO_3, CH_3OH/CH_2Cl_2, RT, 3h (viii) 5-bromothiophene-2-carboxaldehyde, TEA, $Pd(PPh_3)_2Cl_2$, CuI, 50 ^oC, 8h (ix) Cyanoacetic acid (PYR-Por-CA or FLU-Por-CA) or malonic acid (PYR-Por-MA or FLU-Por-MA), $CHCl_3/CH_3CN$ (3:1), piperidine, reflux, 8h.

Figure 2: Synthetic scheme.

experimental procedure and analytical data *See Supporting information*). We have adopted the Lindsey method for the synthesis of the unsymmetrical porphyrin (**3**).[31] The donors, polycyclic aromatic hydrocarbons such as either pyrene or fluorene, were introduced at the *–meso* position *via* Suzuki-Miyura cross-coupling with the corresponding donor boronic acid pinacol ester and mono brominated porphyrin (**3**). Thiophene moiety with rigid ethynyl linker was introduced *via* Sonogashira cross-coupling reaction of the corresponding TMS(Trimethysilylacetylene) deprotected porphyrin (either **9a** or **9b**) with 5-bromo thiophene carboxaldehyde. Finally, presence of hexyloxy substituents on *10-* and *20-meso* phenyl rings of the porphyrin macrocycle is to increase the solubility of the porphyrin and was also expected to minimise charge recombination.[26] The presence of the thiophene group is to enhance the molar absorption coefficient, bathochromically shift the absorption and increase the excited state life time.[32] Moreover, some of the thiophene based organic D-π-A sensitizers are shown to improve the open circuit voltage and enhance the efficiency up to 7%.[33,34] All new unsymmetrical porphyrins are characterized by various spectroscopic techniques. The MALDI-TOF MS mass spectra of each compound displays peaks at **PYR-Por-CA**: 1246 [(M-H)$^+$], **PYR-Por-MA**: 1264 [(M-2H)$^+$], **FLU-Por-CA**: 1381

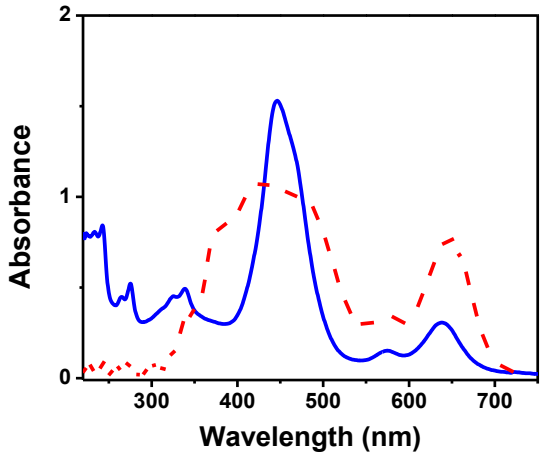

Figure 3: UV–Vis absorption spectra of **PYR-Por-CA** (——) in CH_2Cl_2 and (-----) adsorbed onto a 2 μm thick TiO_2 film.

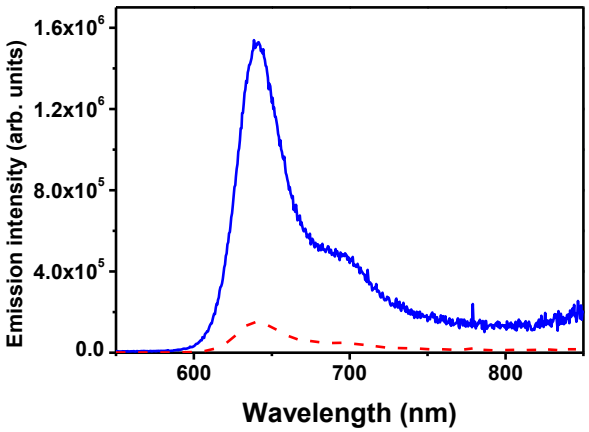

Figure 4: Fluorescence spectra of **PYR-Por-CA** (——) in CH_2Cl_2 and (------) adsorbed onto a 2 μm thick TiO_2 film. The excitation wavelength λ_{ex} = 440 nm.

$[(M+H)^+]$ and **FLU-Por-MA**: 1400 $[(M+H)^+]$, which ascribe to the presence of the molecular ion peak (*See Supporting information*).

The electronic absorption spectra of typical metallo porphyrins are having an intense Soret band at around 420 nm, which is which is an $a_{1u}(\pi)/e_g(\pi^*)$ electronic transition, assigned to the second excited state (S_2) and two less-intense Q bands (500-700 nm) originating from $a_{2u}(\pi)/e_g(\pi^*)$ electronic transition, attributed to the first excited state (S_1). The absorption spectra of all four sensitizers have been measured in dichloromethane solvent and representative absorption spectra of **PYR-Por-CA** depicted in Figure 3 and the corresponding absorption maxima and molar extinction coefficients are given in Table 1. Figure 3 and Table 1 suggests that the absorption peaks in the ultra violet region i.e., between 230-380 nm region belong to the absorption of donor **PAH** group in all four sensitizers and it is not much altered, when compared to its isolated donor molecules. In contrast, a split in the Soret band was observed in both fluorene derivatives *i.e.*, **FLU-Por-CA** and **FLU-Por-MA** (*See* supporting information). Both Soret and Q bands of all four sensitizers are broadened and red-shifted in comparison with ZnTTP, which could be attributed to the reduced molecular symmetry, extended-π conjugation *via* ethynyl linker and also due to electronic communication between the aromatic hydrocarbon donors/thiophene with the porphyrin macrocycle. The broadening of absorption bands is more pronounced in sensitizers with malonic acid anchoring group sensitizers (**PYR-Por-MA** & **FLU-Por-MA**) than the corresponding cyanoacrylic acid derivatives (**PYR-Por-CA** & **FLU-Por-CA**) (*See Supporting information*). Similarly, the sensitizers having pyrene derivatives are more bathochromically shifted when compared to their fluorene derivatives, which may be due to more electron releasing nature of the pyrene moiety.[25,35] Figure 3 also displays the absorption spectrum of **PYR-Por-CA** adsorbed onto 2 μm thick TiO_2 electrode which is similar to that of the solution spectra but exhibits a small red shift. This may be due to the anchoring of carboxylic protons of porphyrin on TiO_2 which releases the proton upon binding to Ti^{4+}.[36]

The emission spectra of all four porphyrin sensitizers were measured at room temperature in dichloromethane solvent and the representative spectrum of **PYR-Por-CA** is illustrated in Figure 4 with the corresponding emission maxima with quantum yields reported in Table 2. From Figure 4 and Table 2, it is clear that the quantum yields of all four sensitizers is enhanced in comparison with reference compound 5,10,15,20-tetraphenyl zinc porphyrin (ZnTPP). The singlet state energies ($E_{0\text{-}0}$) of all four sensitizers, estimated from excitation and emission spectra are presented in Table 2. No emission spectra are observed for the porphyrin sensitizers adsorbed

Table 1: UV-visible absorption and electrochemical data.

Compound	Absorption, λ_{max}, nm (log ε, M^{-1} cm^{-1})[a]							Potential V vs. SCE[c]			
	Porphyrin Bands			Donor PAH Bands[c]				Reduction		Oxidation	
PYR-Por-CA	447 (5.60)	575 (4.13)	639 (4.40)	339 (4.60)	326 (4.50)	275 (4.60)	234 (4.70)	-1.05, -1.62	-1.34,	0.76, 1.50	1.12,
PYR-Por-MA	468 (5.11)	580 (4.02)	654 (4.41)	339 (4.50)	326 (4.50)	275 (4.50)	234 (4.70)	-1.26, -1.60	-1.50	0.64, 1.29,	1.06,
FLU-Por-CA	444 (5.21)	569 (4.17)	638 (4.51)	267 (4.61)	308 (4.50)			-1.14, -1.70	-1.47,	0.79, 1.47	1.09,
FLU-Por-MA	448 (5.33)	572 (4.20)	632 (4.41)	266 (4.62)	309 (4.61)			-0.98, -1.51	-1.35,	0.66,	1.27,

[a]Solvent CH_2Cl_2, Error limits: λ_{max}, ± 1 nm, log ε, ± 10%. [b]D = Pyrene or Fluorene. [c]CH_2Cl_2, 0.1 M TBAP; Glassy carbon working

Table 2: Fluorescence data[a] and fluorescence decay parameters.

Compound	λ_{em}, nm[a] (ϕ,)	τ, ns (A%)[b]	$E_{0\text{-}0}$ (eV)[c]	E_{ox}^{*}
PYR-Por-CA	651 (0.069)	0.82 (80.03) 0.09 (19.97)	1.92	-1.16
PYR-Por-MA	688 (0.060)	0.97 (63.62) 1.94 (36.38)	1.85	-1.21
FLU-Por-CA	662 (0.070)	0.71 (78.15) 1.84 (21.85)	1.91	-1.12
FLU-Por-MA	639 (0.078)	0.95 (43.50) 2.00 (56.42)	1.95	-1.29

[a]Error limits: λ_{ex}, ±2 nm; ϕ, ±10%. [b]All lifetimes are in nanoseconds (ns). ‡ Error limits of τ ~ 5%. [c] Error limits: ±0.05 eV. [d]Excited state oxidation potentials are calculated by using $E^{*} = E_{1/2(OX)}\text{-}E_{0\text{-}0}$.

onto 6 μm thick TiO_2 layer as a consequence of electron injection from excited singlet state of porphyrin into the conduction band of TiO_2. The singlet excited-state life-times of all four unsymmetrical porphyrins were measured in DCM solvent (λ_{ex} = 440 nm & λ_{em} = 650 nm) and were found to be 0.82, 0.97, 0.71 & 0.95 ns for **PYR-Por-CA**, **PYR-Por-MA**, **FLU-Por-CA** & **FLU-Por-MA**, respectively (*See* Supporting information). In all four cases the excited state life-time was quenched when adsorbed onto 2 μm thick TiO_2 layer.

With a view to evaluate the HOMO-LUMO levels of the porphyrin sensitizers, we have performed the electrochemistry by using cyclic and differential pulse voltammetric techniques in dichloromethane solvent. The redox potentials were determined from half-wave potentials ($E_{1/2}$) (E_{OX}-E_{red})/2) by cyclic voltammetry (CV) or peak potentials (E_p) by differential pulse voltammetry (DPV). The redox potential data are presented in Table 1. Each new porphyrin sensitizer undergoes three reductions and either two or three oxidations under the experimental conditions employed. Wave analysis suggested that, both oxidation and reduction reactions are either quasireversible or totally irreversible. The first two oxidation processes belongs to the porphyrin macrocycle that generates π-cation radical and the dication and the third oxidation belongs to the polycyclic aromatic hydrocarbon moiety in all four investigated sensitizers. The data presented in Table 1, suggest that the sensitizers with cyanoacrylic acid group are more difficult to oxidize than the corresponding sensitizers with malonic acid group. This is due to the more electron withdrawing nature of cyanoacrylic acid group. The excited state oxidation potential of all four porphyrin sensitizers (Table 1) was found to be more negative than the energy level of conduction band edge of TiO_2 (-0.8 V vs. SCE)[37] and E_{OX} energy level is more positive than the redox potential of iodine/iodide system (0.2V vs. SCE)[38] for these dyes.

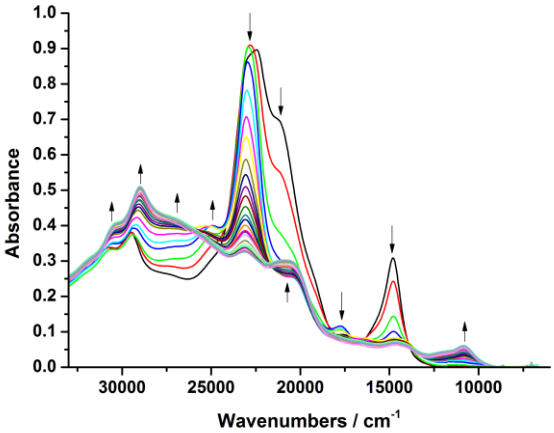

Figure 5: *In-Situ* UV-Vis spectral changes of **PYR-Por-CA** at an applied potential of 1.0 V.

In DSSC, the sensitizer promotes an electron to the excited state by absorbing a photon and then injects the excited electron to the semiconductor on an ultra-rapid time scale. To gain insight into the electronic properties of the oxidized species of the porphyrin sensitizers, we carried out a spectro-electrochemical study.[39] Figure 5 shows spectral changes of **PYR-Por-CA** under applied potential. During the controlled potential oxidation of **PYR-Por-CA** at 1.00 V, the absorption of both Soret and Q band decreases in intensity without shift, while a new band appeared at 11000 cm^{-1}. Prolonged oxidation at 1.0 V, results in further decrease in intensity of the Soret band and disappearance of the Q bands. On the other hand, bands in the spectral region corresponding to the donor pyrene moiety show an increase in spectral intensity. During this process, isosbestic points were initially observed, indicating that oxidation gives a single product, however at longer times these were lost. These characteristic changes indicate the formation of the porphyrin cation radical.[40] The electrochemical oxidation is not fully reversible under these conditions as the porphyrin cation generated at +1.00 V can't be fully recovered to its neutral form when the applied potential was changed to +0.2 V. Thus, although the oxidation was observed to be reversible during cyclic voltammetry, during the longer timescale of the spectroelectrochemical study some degradation was observed. The species after spectroelectrochemistry still displays features characteristic of a porphyrin, however some chemical change to the substituent groups has presumably occurred. We note that during operation of the solar cell, the sensitizer remains in the oxidised form for a much shorter time and indeed, **PYR-Por-CA** shows greater oxidative stability during spectroelectrochemistry than the well-known Ru-sensitizer N719 under similar conditions.[40] Similar spectral changes are observed in **PYR-Por-MA**, **FLU-Por-CA** & **FLU-Por-MA** sensitizers (*See Supporting information*).

Quantum Mechanical Calculations

In order to obtain insight on the effect of differing donor (pyrene or fluorene) and acceptor (CA or MA) groups on the electrochemical, optical and geometrical properties of these new porphyrin

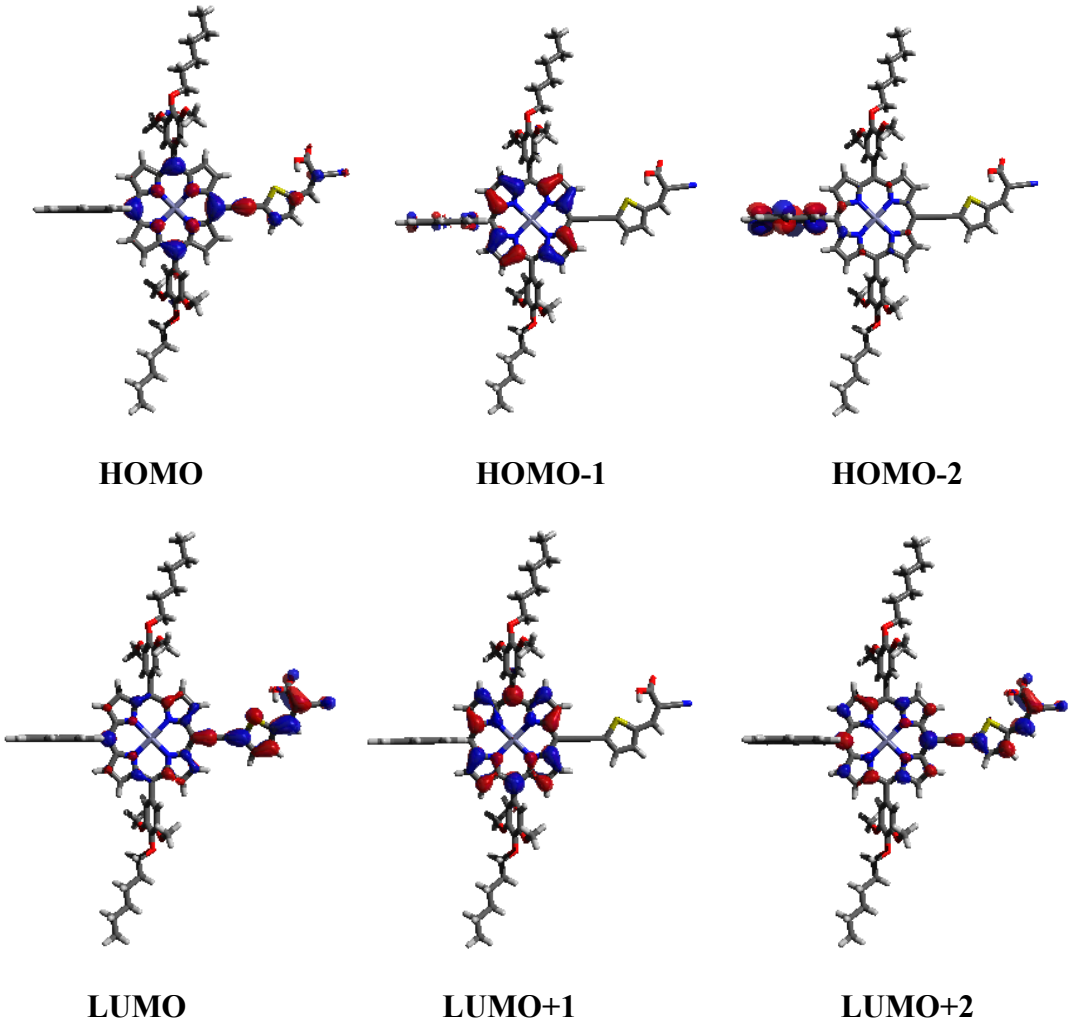

Figure 6: Frontier orbitals of **PYR-Por-MA** calculated using B3LYP/6-31G(d) within dichloromethane PCM.

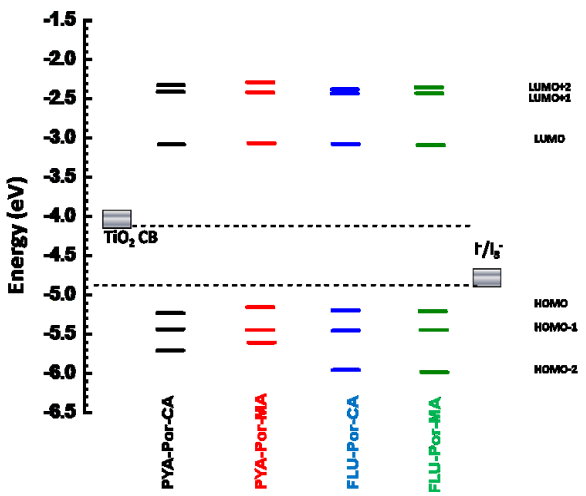

Figure 7: Energy level diagram of D-π-A dyes.

sensitizers, we have performed TD-DFT calculations using B3LYP/6-31G(d) level indichloromethane polarisable-continuum model solvent phase. The molecular orbital analysis of the frontier orbitals of **PYR-Por-CA** is illustrated in Figure 6 while their energy levels are summarized in Table 3. The electron distribution pattern in Figure 6 suggests that the first two HOMOs are essentially porphyrin ring centred with a slight electron delocalization onto the donor pyrene and on the thiophene part of the anchoring group whereas in the HOMO-2, the delocalization was mainly on the donor pyrene along with a contribution from the macrocyclic ring. In contrast the electron density of the LUMO level was mainly localized on the thiophene-cyanoacrylic acid moiety, anchoring group and on the ethynyl linker with a considerable contribution from the porphyrin ring as well. In contrast, for LUMO+1 the electron density was exclusively distributed on the porphyrin ring and for LUMO+2 there was delocalization of electron density on both porphyrin and the ethynyl thiophene linker. The above discussion suggests that the porphyrin unit is mainly responsible for the first oxidation process, although with a noticeable contribution from

Table 3: Percentage contributions from component parts of **PYR-Por-CA** to selected molecular orbitals. Also quoted are the calculated energies for these molecular orbitals.(Ar-based = trimethoxyaryl unit; S-based = thiophene-cyanoacetic acid unit)

MO	MO energy / eV	% Contribution from				
		Zn-based	Porphyrin- based	Pyrene- based	S-based	Ar-based
HOMO-2	-5.52	0.01	15.66	82.80	0.16	1.37
HOMO-1	-5.47	0	79.93	12.91	0.04	7.12
HOMO	-5.22	0.84	62.12	3.17	23.46	10.41
LUMO	-3.09	0.16	32.48	1.86	63.91	1.59
LUMO+1	-2.44	0.23	88.60	1.42	0	9.75
LUMO+2	-2.37	0.14	53.27	3.21	41.23	2.15

the thiophene adjacent to the anchoring group. Similarly, the first reduction process in each of the reported porphyrins was contributed by charge delocalization on both the ethynyl thiophene acrylic acid groups and the porphyrin macrocyclic ring. The pyrene unit plays a negligible role in the frontier orbitals suggesting its potential role as an electron donating unit is not realised in practice, consistent with little change in redox potential between fluorene and pyrene analogues. This may be detrimental in terms of charge separation following electron transfer to the TiO_2, since a noticeable component of the positive charge density on the dye will be distributed close to the TiO_2 which can promote charge recombination. Figure 7 depicts the energy level diagram of D-π-A porphyrins with the conduction band (CB) of TiO_2 as well as redox energy of I^-/I_3^-. As suggested in the Figure 7, all four new porphyrin sensitizers should be capable of injecting electrons to the CB of TiO_2 upon excitation. More importantly, electron injection from the sensitizers to TiO_2 should be more favourable for **PYR-Por-MA** than the other sensitizers owing to the higher LUMO levels.

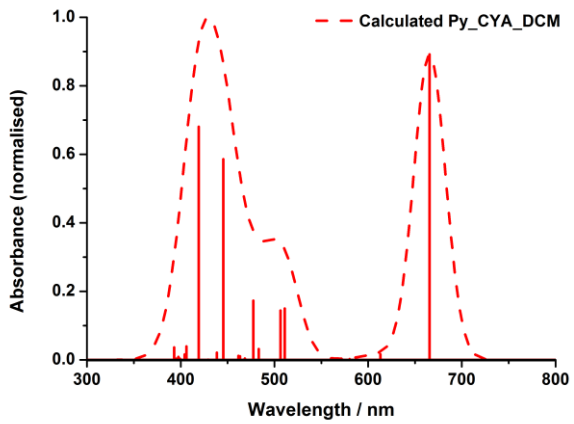

Figure 8: The red dash curve is the calculated spectrum of **PYR-Por-CA** in dichloromethane and the solid columns are the calculated electronic transitions.

In Figure 8 we report the calculated absorption spectra of **PYR-Por-CA** in dichloromethane solvent. All calculated electronic transitions energies, along with their oscillator strengths and molecular orbital compositions of dyes are summarized in supporting information. In general, the calculations show excellent agreement with the experimental spectra, although the Q-band, assigned to the HOMO-LUMO transition (>80%), shows a higher than expected intensity.

Photovoltaic Measurements

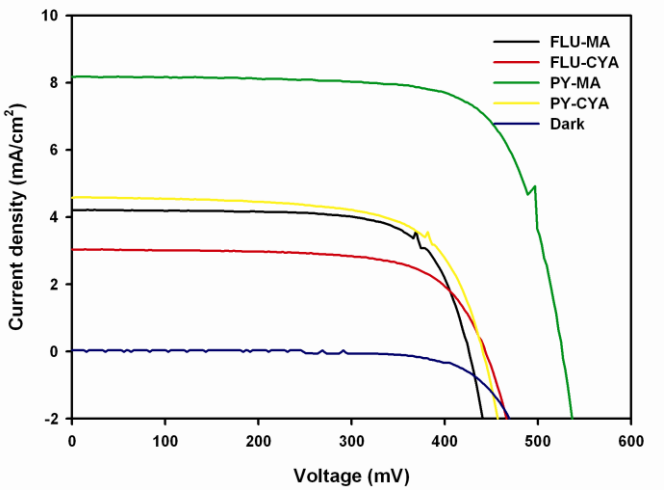

Figure 9: J−V characteristics of DSSCs constructed with different porphyrin sensitizers under 1 sun illumination

Figure 9 shows the performance of the DSSCs of different sensitizers on the basis of their steady-state current−voltage characteristics. Table 4 summarizes the key cell parameters for DSSCs as a function of different porphyrin sensitizers. DSSC parameters are significantly influenced by the porphyrin sensitizers. The maximum conversion efficiency has been achieved for the cells sensitized with **PYA-Por-MA**. It shows increased J_{sc} and V_{oc} effects

Table 4: Cell Parameters of DSSCs Made with different sensitizers (1 sun illumination)

Compound	V_{OC}[a] (mV)	J_{SC}[a] (mA/cm^2)	ff[a] (%)	η (%)
PYA-Por-CA	439	4.59	67.15	1.35
PYA-Por-MA	525	8.19	73.21	3.14
FLU-Por-CA	443	3.04	68.92	0.92
FLU-Por-MA	424	4.21	71.88	1.28
N719[48]	622	18.1	73.79	8.35

[a]Error limits: J_{SC}: ±0.20 mA/cm^2, V_{OC} = ±30 mV, ff = ±0.03.

in the frontier orbitals. However, the overall conversion efficiency is less than the controlled cells made with standard N719 sensitizer. The reason for the decreased efficiency compared to the previously reported acene modified dyes can be deduced as follows. The flaccidity of the acrylic bond causes the dye molecule anchored on TiO_2 to be inclined with respect to the adjacent dye molecule, consequently reducing the extent of dye adsorption on TiO_2 (FF) and henceforth results in a decreased IPCE and current density values.[42] Moreover there is also a chance of increased recombination rate at the TiO_2/ electrolyte interface, due to the possibility of halogen bonding between Iodine in the electrolyte and some electron rich segments like the sulfur atom in the thiophene moiety.[43] The presence of long side chains may be an added advantage to minimize dye aggregation but still they may lead to surface blocking, resulting in low dye uptake.[44,45] The reduced V_{oc} values of certain zinc porphyrin dyes may be due to faster recombination rate between TiO_2 electrons and the acceptor species in the I^-/I_3^- redox electrolyte and also by means of other deactivation pathways which competes and lowers the electron injection efficiency.[45] The introduction of twisted spacer as an alternative to rigid benzoic acid anchoring group may interrupt the overall conjugation in the dye molecule and hence weakens the ICT interaction and also replacing a phenyl spacer with a thiophene moiety may also lead to decrease in the total absorption cross-section by half which will consequently lead to poor photovoltaic performance.[43,46]

Thermal Stability

Finally, we have studied the thermal stability of these porphyrin sensitizers by using thermogravimetric analysis. This thermal stability is essential for roof top applications of DSSC devices. It is well known in the literature that tetraphenyl porphyrin and its metallo derivatives are thermally stable up to 400 ^oC. Figure 10 shows the thermal behaviour of **PYR-Por-CA**. From the figure it is clear that the sensitizer **PYR-Por-CA** is stable up to 250 ^oC. The initial weight loss (~2%) observed between 200 to 250 ^oC is attributed to the removal of the carboxyl group. A similar trend in thermal stability was also obtained in other sensitizers of this series

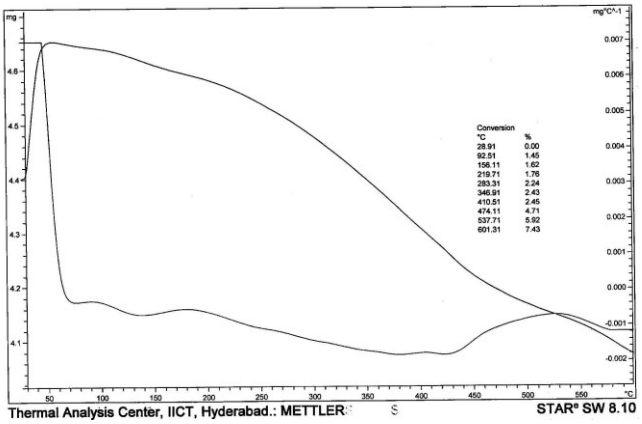

Figure 10: TG/DTG curves of **PYR-Por-CA** with heating rate of 10 ^oC min^{-1} under Nitrogen atmosphere.

(*See Supporting information*). It is clear from the thermal data that these dyads are highly durable for longstanding outdoor applications.

Conclusions

In conclusion, we have designed four unsymmetrical zinc porphyrins based on D-π-A approach for DSSC applications. Both Soret and Q band absorption of all four sensitizers are broadened and red-shifted. The emission maxima and excited state life-time were quenched, when adsorbed onto nanocrystalline TiO_2. Electrochemical and spectro-electrochemical properties suggest that first oxidation is localized on the porphyrin centre. Up on photosensitization of nanocrystalline TiO_2, the pyrene substituted sensitizers have shown efficiency of up to 3.14%. The reason may be due to more electron releasing nature of pyrene derivatives than the corresponding fluorrne derivatives. This result the Soret band absorption is more red-shifted in case of pyrene derivatives as it can harvest more sunlight and more favorable conditions for injection of electron from excited state of sensitizer to the TiO_2 conduction band. However for exact reason, one has to do the dynamic studies of these sensitizers in detail and also impedance spectroscopy. Such studies are currently in progress.

Notes and references

† Electronic Supplementary Information (ESI) available: [Detailed experimental procedure, absorption and emission spectra, fluorescence decay curves, spectro-electrochemical, HOMO-LUMO energy levels information available]. See DOI: 10.1039/b000000x/

1. T. Ameri, P. Khoram, J. Min, and C. J. Brabec, *Adv. Mater*. 2013, **25**, 4245-4266.
2. M. E. Ragoussi, M. Ince and T. Torres, *Euro. J. Org. Chem*. 2013, DOI: 10.1002/ejoc.201301009.
3. L. L. Li and E. W. -G. Diau, *Chem. Soc. Rev*. 2013, **42**, 291-304.
4. H. M. Upadhyaya, S. Senthilarasu, M. –H. Hsu, D. K. Kumar, *Solar Energy Materials & Solar Cells* 2013, **119**, 291-295.
5. L. Giribabu and R. K. Kanaparthi, *Current Sci*. 2013, **104**, 847-855.

6. R. K. Kanaparthi, J. Kandhadi and L. Giribabu, *Tetrahedron* 2012, **68**, 8383-8393.
7. M. G. Walter, A. B. Rudine and C. C. Wasmer, *J. Porphyhrins & Phthalocyanines* 2010, **14**, 759-792.
8. N. Robertson, *Angew Chem. Int. Ed*. 2006, **45**, 2338-2345.
9. B. O'Regan, and M. Graetzel, *Nature* 1991, **353**, 737-740.
10. M.K. Nazeeruddin, P. Pechy, T. Renouard, S.M. Zakeeruddin, R. Humphry-Baker, P. Comte, P. Liska, L. Cevery, E. Costa, V. Shklover, L. Spiccia, G.B. Deacon, C.A. Bignozzi, and M. Gratzel, *J. Am. Chem. Soc*. 2001, **123**, 1613–1624.
11. P. Wang, S. M. Zakeeruddin, P. Comte, R. Charvet, R. Humphry-Baker, and M. Gratzel, J. Phys. Chem B, 2003, **107**, 14336-14341.
12. L. Han, A. Islam, H. Chen, C. Malapaka, B. Chiranjeevi, S. Zhang, X. Yang, and M. Yanagida, *Energy & Environ. Sci*. 2012, **5**, 6057-6060.
13. L. Giribabu, R. K. Kanaparthi, and V. Velkannan, *Chem. Record* 2012, **12**, 306-328.
14. L. R. Milgrom, The colours of life: An introduction to the Chemistry of Porphyrins and Related Compounds, Oxford University Press: New York, 1997.
15. P. S. Reeta, J. Kandhadi, L. Giribabu, *Tetrahedron Lett*. 2010, **51**, 2865-2867.
16. M. W. Lee, D. Lee, W. N. Yen, and C. Y. Yeh, *J. Macromol. Sci., Part A*, 2009, **46**, 730–737.
17. S. Eu, S. Hayashi, T. Umeyama, Y. Matano, Y. Araki, and H. Imahori, *J. Phys. Chem. C*, 2008, **112**, 4396–4405.
18. L. Giribabu, C. V. Kumar, M. Raghavender, K. Somaiah, P. Y. Reddy, and P. V. Rao, *J. Chem. Sci.* 2008, **120**, 455-462.
19. W. M. Campbell, K. W. Jolley, P. Wagner, K. Wagner, P. J. Walsh, K. C. Gordon, L. Schmidt-Mende, M. K. Nazeeruddin, Q. Wang, M. Gratzel, D. L. Officer, *J. Phys. Chem.C* 2007, **111**, 11760-11762.
20. L. Giribabu, C. V. Kumar, and P. Y. Reddy, *J. Porphyrins & Phthalocyanines*, 2006, **10**, 1007-1016.
21. J. R. Durrant, S. A. Haque, and E. Palomares, *Chem. Commun*., 2006, **31**, 3279–3289.
22. R. B. Ambre, G. F. Chang, M. R. Zanwar, C. F. Yao, E. –W. G. Diau, and CH. Hung, *Chem. Asian J*. 2013, **8**, 2144-2153.
23. N. M. Reddy, T. –Y. Pan, R. C. Rajan, B. –C. Guo, C. –M. Lan, E. –W. G. Diau, and C. –Y. Yeh, *PhyChemChemPhy*, 2013, *15*, 8409-8415.
24. M. S. Kang, S. H. Kang, S. G. Kim, I. T. Choi, J. H. Ryu, M. J. Ju, D. Cho, J. Y. Lee and H. K. Kim, *Chem. Commun*. 2012, **48**, 9349-9351.
25. C. –L. Wang, Y. –C. Chang, C. –M. Lan, C. –F. Lo, E. W. –G. Diau and C.-Y. Lin, *Energy Environ. Sci*. 2011, **4**, 1788-1795.
26. A. Yella, H. –W. Lee, H. N. Tsao, C. Yi, A. K. Chandiran, M. K. Nazeeruddin, W. –W. G. Diau, C. –Y. Yeh, S. M. Zakeeruddin, M. Grätzel, *Science* 2011, **334**, 629-634.
27. T. Bessho, S. M. Zakeeruddin, C. –Y. Yeh, E. W.-G. Diau, and M. Grätzel, *Angew. Chem., Int. Ed. Engl.,* 2010, **49**, 6646–6649.
28. C. L. Wang, Y. C. Chang, C. M. Lan, C. F. Lo, E. W. Guang Diau and C.Y. Lin, *Energy Environ. Sci.*, 2012, **5**, 6933–6940.
29. H. –P. Lu, C. –L. Mai, C. –Y. Tsia, S. –J. Hsu, C. –P. Hsieh, C. –L. Chiu, C. –Y. Yeh and E. –W. Diau, *Phys. Chem. Chem. Phys*. 2009, **11**, 10270-10274..
30. N. Xianga, X. Huang, X. Feng, Y. Liu, B. Zhao, L. Deng, P. Shen, J. Fei, and S. Tan, *Deys & Pigments* 2011, **88**, 75-83.
31. B. J. Littler, M. A. Miller, C. –H. Hung, R. W. Wagner, D. F. O'Shea, P. D. Boyle, and J. S. Lindsey, *J. Org. Chem*, 1999, **64**, 1391-1396.
32. R. Ziessel, P. Bäuerle, M. Ammann, A. Barbieri, and F. Barigelletti, *Chem. Commun.* 2005, 802-804.
33. V. V. Diev, C. W. Schlenker, K. Hanson, Q. Zhong, J. D. Zimmerman, S. R. Forrest, and M. E. Thompson, *J. Org. Chem*, 2012, **77**, 143-159.
34. M. Pasini, S. Destri, W. Porzio, C. Botta, and U. Giovanella, *J. Mater. Chem*. 2003, **13**, 807–813.
35. Ch. –H. Wu, T. –Y. Pan, S. –H. Hong, Ch. –L. Wang, H. –H. Kuo, Y. –Y. Chu, E. W. Guang Diau and Ch. –Y. Lin. *Chem. Commun*., 2012, **48**, 4329-4331.
36. M.K. Nazeeruddin, R. Splivallo, P. Liska, P. Comte, and M. Grätzel, *Chem. Commun*., 2003, 1456-1457.
37. X. L. Zhang, F. Huang, A. Nattestad, K. Wang, D. Fu, A. Mishra, P. Bäuerle, U. Bach, and Y. Cheng, *Chem. Commun*., 2011, **47**, 4808-4810.
38. A. Hagfeldt, and M. Gratzel, *Chem. Rev*. 1995, **95**, 49-68.
39. N. Cai, S. –J. Moon, L. Cevey-Ha, T. Mohel, R. Humphry-Baker, P. Wang, S. M. Zakeeruddin, and M. Gratzel, *Nano Lett*. 2011, **11**, 1452-1456.
40. Y.-S. Chen, C. Li, Z.-H. Zeng, W.-B. Wang, X.-S. Wang, and B.-W. Zhang, *J. Mater. Chem.* 2005, 15, 1654-1661
41. K. L. McCall, J. R. Jennings, H. Wang, A. Morandeira, L. M. Peter, J. R. Durrant, L. J. Yellowlees, J. D. Woollins, and N. Robertson, *J. Photochem, Photobiol. A,* 2009, **202**, 196-204.
42. C. –W. Lee, H. –P, Lu, C. –M, Lan, Y. –L, Huang, Y, -R. Liang, W. –N. Yen, Y. –C. Liu, Y. –S. Lin, E. W. –G. Diau, and C. –Y. Yeh, *Chem. Eur. J.* 2009, **15**, 1403-1412.
43. Y. C. Chang, C. L. Wang, T.Y. Pan, S. H. Hong, C. M. Lan, H. H. Kuo, C. Fu Lo, H. Y. Hsu, C. Y. Lin and E. W. Guang Diau, *Chem. Commun.*, 2011, **47**, 8910-8912.
44. T. Marinado, K. Nonomura, J. Nissfolk, M. K. Karlsson, D. P. Hagberg, L. Sun, S. Mori and A. Hagfeldt, *Langmuir*,2010, **26**, 2592–2598.
45. W. H. Liu, I. C. Wu, C. H. Lai, C. H. Lai, P. T. Chou, Y. T. Li, C. L. Chen, Y.Y. Hsu and Y. Chi, *Chem. Commun*., 2008, 5152–5154.
46. M. Liang and J. Chen, *Chem. Soc. Rev.*, 2013, **42**, 3453-3488.
47. M. J. Griffith, K. Sunahara, P. Wagner, K. Wagner, G. G. Wallace, D. L. Officer, A. Furube, R. Katoh, S. Mori and A. J. Mozer, *Chem. Commun.,* 2012, **48**, 4145–4162.
48. (N719 = bis(tetrabutylammonium) *cis*-di(thiocyanato)-bis(4,4′-dicarboxy-2,2′-bipyridine)ruthenium(II)) Z. –S. Wang, H. Kawauchi, T. Kashima and H. Arakawa. Coord. Chem. Rev. 2004, 248, 1381-1389.

